

## Pinning of the domain walls of the cluster spin-glass phase in the low-temperature-tetragonal phase of $\text{La}_{2-x}\text{Ba}_x\text{CuO}_4$

F. Cordero

*CNR, Istituto di Acustica "O.M. Corbino," Via del Fosso del Cavaliere 100, I-00133 Roma, Italy  
and Unità INFN-Roma1, P. le A. Moro 2, I-00185 Roma, Italy*

A. Paolone and R. Cantelli

*Università di Roma "La Sapienza," Dipartimento di Fisica,  
and Unità INFN-Roma 1, P. le A. Moro 2, I-00185 Roma, Italy*

M. Ferretti

*Università di Genova, Dipartimento di Chimica e Chimica Industriale,  
and Unità INFN-Genova, Via Dodecanneso 31, I-16146 Genova, Italy*

(Received 25 May 2001; published 16 August 2001)

We compare the low frequency ( $\sim 1$  kHz) anelastic spectra of  $\text{La}_{2-x}\text{Sr}_x\text{CuO}_4$  and  $\text{La}_{2-x}\text{Ba}_x\text{CuO}_4$  at  $x = 0.03$  and  $0.06$  in the temperature region where the freezing into the cluster spin-glass (CSG) phase occurs and is accompanied by an increase of the acoustic absorption. The dependence of the amplitude of the anelastic relaxation on doping is explained in terms of movement of the domain walls (DW) in the CSG phase between the Sr (Ba) pinning points. The LSCO sample at  $x = 0.06$  transforms into the LTT structure below 40 K and the amplitude of the anelastic anomaly related to the CSG state is 7 times smaller than expected, indicating pinning of the DW which run parallel to the LTT modulation. Such DW can be identified with the stripes of high hole density, and the present measurements show that they are mobile between the Sr (Ba) pinning points down to few K, but become static in the presence of LTT modulation also far from the condition  $x = \frac{1}{8}$  for commensurability between stripe and lattice periodicities.

DOI: 10.1103/PhysRevB.64.132501

PACS number(s): 74.25.Ld, 62.40.+i, 74.72.Dn

The charge/spin inhomogeneities in the high- $T_c$  superconductors (HTS), related oxides and more recently in manganites, have been arising ever growing interest. The HTS are composed of antiferromagnetic (AF) insulating  $\text{CuO}_2$  planes that are made conducting by injecting holes through heterovalent cation doping or introduction of excess O (for a review see, e.g., Ref. 1). Such mobile charges are not homogeneously distributed; early nuclear quadrupole resonance (NQR) experiments suggested that in underdoped nonsuperconducting  $\text{La}_{2-x}\text{Sr}_x\text{CuO}_4$  (LSCO) when  $x > 0.02$  the holes segregate into domain walls for AF domains;<sup>2</sup> below  $T_g(x) \approx (0.2 \text{ K})/x$  these domains freeze into a cluster spin-glass (CSG) state with random directions of the staggered magnetization.<sup>1,3,4</sup> This phenomenology has recently been found in other HTS.<sup>5</sup> On the other hand, on the basis of EXAFS and diffraction experiments, it was proposed that the  $\text{CuO}_2$  planes of the HTS are corrugated according to two different patterns coexisting in a striped fashion, with the mobile holes confined to the low-temperature orthorhombic (LTO) pattern.<sup>6</sup> The stripelike ordering of the charge walls separating AF domains<sup>3,4,7</sup> appears both in the magnetic scattering from the spin correlations and as weak Bragg reflections,<sup>7</sup> when sufficient long-range order is established. In LSCO the ordering is dynamic and incommensurate with the lattice, with a modulation wave vector shifted from the AF wave vector by  $\delta \approx x$ . Such a linear relationship between incommensurability  $\delta$  and doping is found to hold for  $0.04 < x < 1/8$ , while  $\delta$  remains locked at  $\sim 1/8$  at higher doping.<sup>8</sup>

The magnetic modulation is parallel to the modulation of the  $\text{CuO}_2$  plane in the LTO structure (at  $45^\circ$  with the Cu-O bonds) for  $x \leq 0.05$ , but becomes parallel to the Cu-O bonds across the metal-insulator transition  $x \geq 0.06$  (Ref. 9). These magnetic neutron diffraction peaks have been recently reported to be elastic,<sup>9</sup> although they could actually be quasi-elastic and therefore correspond to fluctuating correlations which are observable only by fast probes such as neutrons.<sup>10</sup> The correlations are considered to be static when the stripe modulation is parallel and commensurate with the lattice modulation;<sup>7,11</sup> this occurs around the doping  $x = 1/8$  in the low-temperature tetragonal (LTT) structure, which is stabilized in samples with large enough disorder of the ion sizes in the La sublattice ( $\text{La}_{2-x-y}\text{Nd}_y\text{Sr}_x\text{CuO}_4$  or  $\text{La}_{2-x}\text{Ba}_x\text{CuO}_4$ ).

The relation between the stripes and superconductivity is debated<sup>11</sup> and it is not yet ascertained whether the stripes are an ingredient of HTS (Refs. 6,12,13) or compete against it.<sup>14</sup> A closely related issue is whether they are static or dynamic,<sup>15,16</sup> and, to our knowledge, their transversal dynamics has never been measured, especially at low frequency. The neutron spectroscopy probes very high frequencies ( $> 10^{11}$  Hz) and can tell whether the observed correlations are quasistatic over that frequency scale; lower frequencies are indirectly probed by NQR or  $\mu\text{SR}$  experiments, e.g., through the fraction of NQR signal which is lost when fluctuations of the order of the NQR frequency ( $10^7$  Hz) make the signal to decay too fast to be

measured.<sup>17,18</sup> The fact that slower probes indicate lower freezing temperatures for the stripe correlations suggests a glassy dynamics,<sup>17,19</sup> but in general it is not distinguished between the dynamics of the single spins or charges and the transversal motion of the stripes. The latter type of motion, which is characteristic of domain walls, can be effectively probed by low frequency susceptibilities,<sup>20,21</sup> and the elastic susceptibility has the advantage over the dielectric and magnetic ones of being practically insensitive to the dynamics of single charges and spins, which otherwise dominate the response.

In order to obtain further insight in this complex interplay of dynamic magnetic and charge ordering and pinning by the lattice, we extended the acoustic spectroscopy measurements of the CSG state in LSCO (Ref. 21) to  $\text{La}_{2-x}\text{Ba}_x\text{CuO}_4$  (LBCO), which has greater tendency to form a stable LTT phase. Two  $\text{La}_{2-x}\text{Ba}_x\text{CuO}_4$  samples and two  $\text{La}_{2-x}\text{Sr}_x\text{CuO}_4$  samples with  $x=0.03$  and  $x=0.06$  were prepared by standard solid state reaction as described in Ref. 22 and cut in bars approximately  $45 \times 5 \times 0.6 \text{ mm}^3$ . The complex Young's modulus  $E(\omega) = E' + iE''$ , whose reciprocal is the elastic compliance  $s = E^{-1}$ , was measured as a function of temperature by electrostatically exciting the lowest three odd flexural modes and detecting the vibration amplitude by a frequency modulation technique. The vibration frequency  $\omega/2\pi$  is proportional to  $\sqrt{E'}$ , while the elastic energy loss coefficient (or reciprocal of the mechanical  $Q$ ) is given by<sup>20</sup>  $Q^{-1}(\omega, T) = E''/E' = s''/s'$ , and was measured by the decay of the free oscillations or the width of the resonance peak. The imaginary part of the dynamic susceptibility  $s''$  is related to the spectral density  $J_\varepsilon(\omega, T) = \int dt e^{i\omega t} \langle \varepsilon(t)\varepsilon(0) \rangle$  of the macroscopic strain  $\varepsilon$  through the fluctuation-dissipation theorem,  $s'' = (\omega V/2k_B T) J_\varepsilon$ .

The spin dynamics can affect  $J_\varepsilon$  through magnetoelastic coupling,<sup>20</sup> namely, an anisotropic strain with principal axes oriented according to the spin orientation. Indeed, it has recently been shown<sup>21</sup> that in LSCO the freezing into the CSG state is accompanied by a steplike increase of the acoustic absorption and a rise of the elastic modulus; the data of  $\text{La}_{2-x}\text{Sr}_x\text{CuO}_4$  with  $x=0.03$  and  $0.06$  are shown in Figs. 1 and 2. The anomaly is observed around or slightly below  $T_g$ , as reported in the literature<sup>23</sup> [ $T_g(x=0.03) \approx 6.7 \text{ K}$  and  $T_g(x=0.06) \approx 3.3 \text{ K}$ ] and deduced from the maxima in the <sup>139</sup>La NQR relaxation rate measured on the same samples.<sup>21,24</sup> The NQR and  $\mu\text{SR}$  experiments measure the spectral density  $J_{\text{spin}}(\omega, T)$  of the spin fluctuations. If the fluctuations occur with a rate  $\tau^{-1}(T)$ , then  $J_{\text{spin}} \propto \tau/[1 + (\omega\tau)^2]$  is peaked at the temperature at which  $\omega\tau = 1$ , and the sharp peaks in the NQR and  $\mu\text{SR}$  relaxation rates indicate the slowing of the spin fluctuations below the measuring angular frequency  $\omega$  ( $\sim 10^7 - 10^8 \text{ Hz}$  in those experiments). The same peak, shifted to lower temperature because of the lower frequency ( $\omega \sim 10^3 - 10^4 \text{ Hz}$ ), could in principle appear also in  $J_\varepsilon$  thanks to the magnetoelastic coupling. However, the steplike  $Q^{-1}(T)$  curves of Fig. 1 cannot be easily identified with the sharp peaks in the NQR rate,<sup>1,2,4,24</sup> and can be attributed to the movement of domain walls separating the antiferromagnetically correlated domains.<sup>21</sup> In this

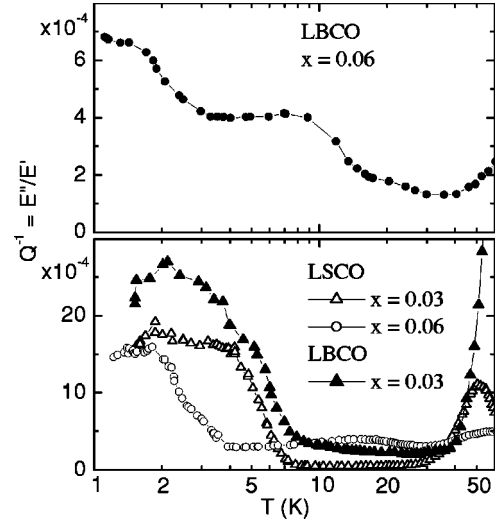


FIG. 1. Elastic energy loss coefficient of LSCO and LBCO at doping  $x=0.03$  and  $0.06$ , measured at  $\sim 1.5 \text{ kHz}$ .

case, the steep rise of the absorption with lowering temperature is determined by the formation of the clusters with frozen AF spin correlations, while the broader shape at lower temperature is due to the wide distribution of the relaxation rates of domain walls with different lengths and mobilities.

The low-doping and low-temperature region of the magnetic phase diagram of LBCO has not been investigated, but the close similarity between the anelastic spectra of LBCO and LSCO in Figs. 1 and 2 indicate that also in LBCO the spins undergo the same freezing processes at practically the same temperatures as in LSCO. The anomalies in the imaginary (Fig. 1) and real parts (Fig. 2) of the dynamic elastic response attributed to the appearance of the CSG state appear below  $7 \text{ K}$  for  $x=0.03$  in both samples and below  $4 \text{ K}$  ( $3 \text{ K}$ ) for  $x=0.06$  in LSCO (LBCO). The similarity between the spectra at  $x=0.03$  is shown in Fig. 3, where both the absorption and real parts of the dynamic response of LSCO and

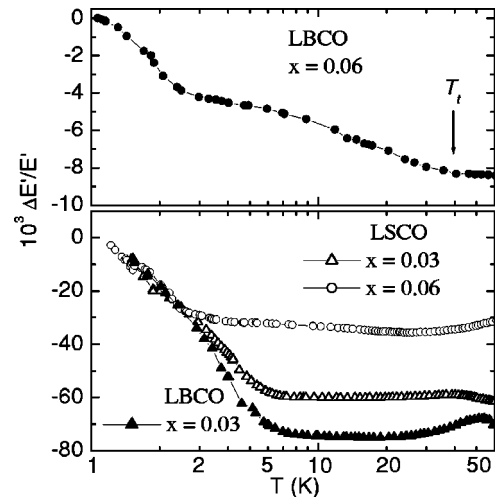


FIG. 2. Relative variation of the Young's modulus of the samples of Fig. 1. The rise of the modulus below  $40 \text{ K}$  in LBCO  $x=0.06$  is attributed to the formation of LTT phase.

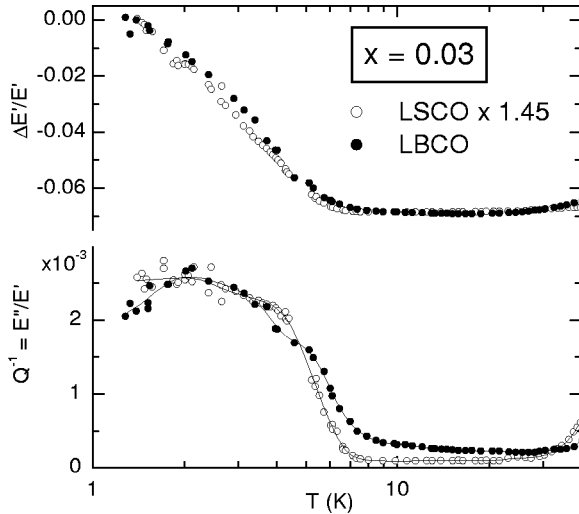


FIG. 3. Comparison between the absorption and real part of the dynamic Young's modulus of LSCO (1.7 kHz) and LBCO (1.2 kHz) at  $x=0.03$  in the region of the freezing into the CSG state. The curves of LSCO have been multiplied by 1.45.

LBCO are plotted together [in all the figures the Young's modulus  $E(T)$  is normalized to the extrapolated  $E(0)$ ]. The data of LSCO practically overlap with those of LBCO if multiplied by 1.45, indicating that the rise of the elastic modulus is determined by the same mechanism producing the absorption. The factor  $\sim 1.5$  can be ascribed to a greater magnetoelastic coupling in the Ba compound, possibly resulting from the slightly different atomic sizes and distances.

We turn now to the dependence of the amplitude of the anelastic effect on doping. For LSCO, the amplitude is a decreasing function of doping, as shown by the open circles of Fig. 4, which includes also data from Ref. 21. We want to show that this trend is in agreement with the proposed mechanism of dissipation (and consequent dispersion in the real part of the modulus<sup>20</sup>) due to the stress-induced change

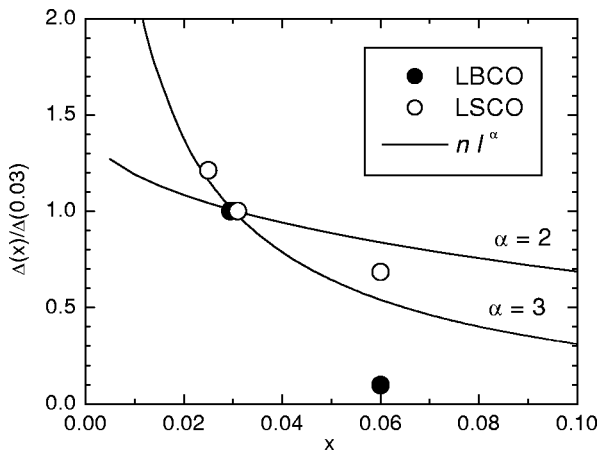


FIG. 4. Intensity  $\Delta$  of the elastic energy loss contribution of the domain walls in the CSG state as a function of doping for LSCO and LBCO; the datum at  $x=0.025$  is from Ref. 21. The continuous lines are obtained from the expression of  $\Delta(x)$  discussed in the text. The data and the curves are normalized at  $x=0.03$ .

of the sizes of domains with differently oriented axes of staggered magnetization.<sup>21</sup> Since the Sr dopants act as pinning points for the DW, their concentration affects not only the density  $n$  of DW but also their mean length  $l$  between pinning points. The relaxation strength  $\Delta$  is expected to be of the form  $\Delta \propto n l^\alpha$  with  $\alpha=3$ , similarly to the case of the motion of dislocations pinned by impurities,<sup>20</sup> or with  $\alpha=2$ , as proposed for the susceptibility due to the motion of DW between ferromagnetic domains.<sup>25</sup>

In Fig. 4 the relaxation strength measured with LSCO is compared with  $\Delta(x) \propto n(x) l^\alpha(x)$  calculated assuming that the Sr atoms above and below a  $\text{CuO}_2$  plane form a square lattice with spacing  $d=1/\sqrt{x}$  in units of the lattice constant  $a$ , and that the DW form a square lattice passing through the Sr atoms; the mean number of free atoms along a DW segment is then  $l=d-1$ , since the two extrema at the Sr pinning points are fixed. In this manner we obtain  $\Delta \propto 2x(1/\sqrt{x}-1)^\alpha$ , which reproduces reasonably well the experimental data of LSCO with  $\alpha \lesssim 3$ . If we assume that the DW run only parallel to one direction, as expected from parallel stripes, then  $n(x)$  is halved, but the dependence on  $x$  remains the same. We conclude that the dependence of the relaxation magnitude on doping is in agreement with what expected from the motion of DW pinned by the Sr atoms.

The case of LBCO at  $x=0.06$  is different, since the amplitude of the step at  $T_g \sim 3.5$  K is 4.8 times smaller than for LSCO (both in the absorption and real parts), and the onset temperature is also slightly lower (Fig. 1). Considering the difference in magnetoelastic coupling, it turns out that the amplitude of the effect in LBCO at  $x=0.06$  is 7 times smaller than expected. This reduction appears clearly in Fig. 4, where all the data are normalized at  $x=0.03$ . The depression of the absorption step in LBCO with  $x=0.06$  has to be attributed to the transformation into the LTT structure below  $T_t \approx 40$  K, which is observed in the anelastic spectrum (Figs. 1 and 2). The LTO-LTT transition has been mainly studied on samples with  $x \approx 0.12$ ,<sup>26</sup> in view of the strong decrease of  $T_c$  around that doping. To our knowledge no data are available for  $0.05 \leq x \leq 0.07$  in LBCO, but our observation of  $T_t \approx 40$  K at  $x=0.06$  is in agreement with the available data<sup>26,27</sup> of  $T_t=0$  K for  $x \leq 0.05$  and  $T_t=50$  K for  $x=0.08$ . The effect of the LTO-LTT transition on the acoustic properties of LBCO has been identified<sup>28</sup> in a small sound attenuation peak and lattice stiffening below  $T_t$  on LBCO samples with  $0.10 \leq x \leq 0.16$ . The amplitude of the stiffening,  $\Delta E/E$ , below  $T_t$  is strongly doping dependent, with a maximum of 0.05 around  $x=0.12$ ,<sup>28</sup> and already lowered to 0.01 at  $x=0.10$ ; the value of 0.004 which we find at  $x=0.06$  is consistent with this trend. Therefore, we identify the increase of  $E'$  below  $T_t \sim 40$  K with the onset of the transformation to the LTT structure. Also LSCO at  $x=0.06$  exhibits similar weak anomalies, which suggest a tendency to the formation of LTT domains also in LSCO, in accordance with the recent high-resolution diffraction experiments.<sup>29</sup> The difference between LSCO and LBCO (or LSCO codoped with Nd) is that in LSCO such domains should be either confined to the twin boundaries or fluctuating, extremely small, and without long range correlation; instead, in LBCO and LSCO codoped with

Nd the diffraction experiments reveal a stable phase with long range order, which can provide a pinning potential for the stripes. Our experiments do not provide any direct information on the extension or topology of the LTT domains, and the elastic anomalies are likely connected with the domain boundaries. It is therefore possible that narrow domains of minority LTT phase in LSCO, with a high perimeter to area ratio, and extended LTT domains in LBCO produce comparable elastic anomalies.

The fact that the anelastic relaxation due to the DW motion in the LTT structure of LBCO is 7 times smaller than in the LTO one of LSCO is a clear indication of pinning of the DW motion within the LTT phase. The pinning of the DW can be attributed to the LTT lattice modulation, with rows of inequivalent O atoms in the  $\text{CuO}_2$  plane (within or out of the plane) along the direction of the Cu-O bonds, irrespective of commensuration effects. Only the walls parallel or nearly parallel to this modulation should be clamped, and therefore from the reduction factor  $\sim 7$  we deduce that about 87% of the DW are parallel to the direction of the Cu-O bonds in the LTT phase (in the assumption of a complete transition to the LTT structure), in agreement with the direction of the magnetic modulation observed by neutron scattering for  $x \geq 0.055$ .<sup>9</sup>

The pinning of the DW of the CSG phase within the LTT structure is not unexpected, since the pinning of the dynamic charge and spin fluctuations into static stripe modulations is well documented for samples with Ba or mixed Nd and Sr substitution with  $x \geq 0.12$ , with modulation wave vector close to the commensurate value  $\frac{1}{8}$  and parallel to the LTT lattice modulation.<sup>7,11</sup> In the present case, however,  $x=0.06$  is far from the condition of commensurability between stripes and lattice. Also, we emphasize that the suppression of the acoustic absorption from the DW motion implies that the pinned DW are static over a time scale longer than

$\omega^{-1} \sim 10^{-3}$  s, which is a much more stringent condition than that for the observation of elastic/quasielastic neutron diffraction peaks.<sup>10</sup> We did not address the frequency dependence of the anelastic spectra,<sup>19</sup> but showed that the hole stripes can be studied similar to other types of domain walls; in particular, their low frequency dynamics can be probed by low frequency susceptibilities. Further work on the same line could provide important information on the dynamics and pinning mechanisms of the stripes in HTS.

Summarizing, we compared the anelastic spectra of Sr- and Ba-substituted La cuprate in the temperature region where the freezing into the cluster spin-glass phase is observed, at doping 0.03 and 0.06. The dependence of the magnitude of the anelastic anomaly on the concentration of Sr has been quantitatively explained in terms of motion of DW which are pinned by the Sr substitutional atoms. The anelastic spectra at  $x=0.03$ , with both LSCO and LBCO having LTO structure, completely overlap with a scaling factor of 1.45, attributed to greater magnetoelastic coupling strength with Ba substitution. Instead, at  $x=0.06$  LBCO transforms into the LTT structure and the acoustic absorption due to the motion of the AF domain walls is strongly reduced, indicating their nearly complete pinning within the LTT structure. The DW between different AF spin clusters are identified with stripes of high hole density, and the rows of inequivalent O atoms in the LTT structure would provide a modulated potential which pins the charge stripes parallel to this modulation. The present measurements show that this clamping effect is strong also in the absence of commensuration between stripe and lattice periodicities (occurring at  $x = \frac{1}{8}$ ).

We thank R.S. Markiewicz for useful discussions. This work has been carried out in the framework of the Progetto di Ricerca Avanzato INFM-SPIS.

<sup>1</sup>A. Rigamonti *et al.*, Rep. Prog. Phys. **61**, 1367 (1998).

<sup>2</sup>J.H. Cho *et al.*, Phys. Rev. B **46**, 3179 (1992).

<sup>3</sup>R.J. Gooding *et al.*, Phys. Rev. B **55**, 6360 (1997).

<sup>4</sup>M.-H. Julien *et al.*, Phys. Rev. Lett. **83**, 604 (1999).

<sup>5</sup>Ch. Niedermayer *et al.*, Phys. Rev. Lett. **80**, 3843 (1998).

<sup>6</sup>A. Bianconi, Solid State Commun. **89**, 933 (1994).

<sup>7</sup>J.M. Tranquada *et al.*, Nature (London) **375**, 561 (1995).

<sup>8</sup>K. Yamada *et al.*, Phys. Rev. B **57**, 6165 (1998).

<sup>9</sup>S. Wakimoto *et al.*, Phys. Rev. B **61**, 3699 (2000).

<sup>10</sup>S. Wakimoto *et al.*, Phys. Rev. B **60**, 769 (1999).

<sup>11</sup>N. Ichikawa *et al.*, Phys. Rev. Lett. **85**, 1738 (2000).

<sup>12</sup>S.A. Kivelson *et al.*, Nature (London) **393**, 550 (1998).

<sup>13</sup>J. Zaanen, Nature (London) **404**, 714 (2000).

<sup>14</sup>S.R. White and D.J. Scalapino, Phys. Rev. B **60**, R753 (1999).

<sup>15</sup>J. Zaanen, Science **286**, 251 (1999).

<sup>16</sup>H.A. Mook and F. Doan, Nature (London) **401**, 145 (1999).

<sup>17</sup>A.W. Hunt *et al.*, Phys. Rev. Lett. **82**, 4300 (1999).

<sup>18</sup>M.-H. Julien *et al.*, Phys. Rev. B **63**, 144508 (2001).

<sup>19</sup>R.S. Markiewicz *et al.*, Phys. Rev. B **64**, 054409 (2001).

<sup>20</sup>A.S. Nowick and B.S. Berry, *Anelastic Relaxation in Crystalline Solids* (Academic Press, New York, 1972).

<sup>21</sup>F. Cordero *et al.*, Phys. Rev. B **62**, 5309 (2000).

<sup>22</sup>M. Napoletano *et al.*, Physica C **319**, 229 (1999).

<sup>23</sup>D.C. Johnston, in *Handbook of Magnetic Materials*, edited by K.H.J. Buschow (North Holland, Amsterdam, 1997), p. 1.

<sup>24</sup>A. Campana *et al.*, Eur. Phys. J. B **18**, 49 (2000).

<sup>25</sup>T. Nattermann *et al.*, Phys. Rev. B **42**, 8577 (1990).

<sup>26</sup>J.D. Axe *et al.*, Phys. Rev. Lett. **62**, 2751 (1989).

<sup>27</sup>J.C. Phillips and K.M. Rabe, Phys. Rev. B **44**, 2863 (1991).

<sup>28</sup>T. Fukase *et al.*, Physica B **165&166**, 1289 (1990).

<sup>29</sup>A.R. Moodenbaugh and D.E. Cox, Physica C **341-348**, 1775 (2000).